

Experimental report

07/09/2022

Proposal: 4-02-587

Council: 4/2020

Title: Intra-Unit-Cell magnetism in optimally doped YBa₂Cu₃O₇-delta

Research area: Physics

This proposal is a continuation of 4-02-541

Main proposer: Dalila BOUNOUA

Experimental team: Lucile MANGIN-THRO

Dalila BOUNOUA

Yvan SIDIS

Victor BALEDENT

Local contacts: Martin BOEHM

Samples: YBa₂Cu₃O_{6.9}

Instrument	Requested days	Allocated days	From	To
THALES	7	7	10/09/2020	16/09/2020
			02/02/2021	08/02/2021

Abstract:

An intra-unit-cell (IUC) magnetism develops below the pseudo-gap (PG) temperature, T^* , in the phase diagram of cuprate superconductors. Since the PG state is considered as being the mother-state out of which superconductivity emerges, it becomes crucial to understand the intrinsic nature of the IUC magnetic correlations and to search for the existence of related fluctuations that could contribute to generate anomalous electronic properties (marginal Fermi liquid, d-wave superconductivity). The present polarized neutron experiment is a continuation of our previous experiment on Thales (Exp. 4-02-541). It will be devoted to the study of the temperature evolution of the IUC magnetic signal, to confirm the observed drop down of the intensity below T_c . We will also search for new low energy magnetic fluctuations around the wave vector associated with the IUC magnetism reported by polarized neutron diffraction. The experiment will be performed on an optimally doped YBa₂Cu₃O_{6.9} single crystal free from the parasitic green phase. To this aim, we ask for 7 days on Thales equipped with cryopad.

Intra-Unit-Cell magnetic in optimally doped $\text{YBa}_2\text{Cu}_3\text{O}_{6.9}$

1/ Scientific case

In the phase diagram of high temperature cuprate superconductors (Fig. 1), the unconventional d-wave superconductivity (SC) emerges out of the mysterious pseudo-gap (PG) phase. One of the properties of PG state is that it exhibits discrete broken symmetries in the same region of the phase diagram over which a partial gap opens in the fermionic spectrum. The discrete broken symmetries are lattice rotation [1-4], interpreted in terms of an (Ising) nematic order, parity (P) [5] and time reversal (T) symmetry [6-9], usually interpreted in terms of loop Current (LC) order [10]. Since the lattice translation (LT) invariance is preserved, the Luttinger's theorem implies that none of these broken symmetries can induce the needed fermionic gap.

An intra-unit-cell (IUC) magnetism that exhibits the same symmetry properties as the so-called LC phase, proposed by C.M. Varma in his theory of the PG [10] has been identified by PND in four cuprate families [11-13]. Considering the hole doping and temperature dependences of the PND signal [8-9,11-13], its specific location in momentum space and the fact that it fulfills the polarization sum rule [14-15], the existence of the IUC magnetism can be taken for granted.

Beyond PND, and despite many attempts, local probes such as NMR, NQR and μSR failed to observe a static magnetic field corresponding the IUC magnetism ([16] and references therein). Indeed, if the ordered moments fluctuate on a timescale shorter than that of the local probe, the local field averages to zero. However, ultra-slow magnetic fluctuations have been recently detected [16-18], with time scale of 5 to 25 ns and a net change at T^* [16]. They are likely associated with an IUC magnetism made of slowly fluctuating finite size domains. In most PND studies, these properties are hidden with the experimental resolution. Only at large hole doping, finite size effects could have been resolved [19].

Following our previous study in nearly optimally doped $\text{YBa}_2\text{Cu}_3\text{O}_{6.85}$ [19] which revealed a quasi-2D and short ranged IUC magnetism, we performed PND measurements away from the IUC magnetic Bragg reflection (1,0,0) [20]. The PND experiment (4-02-541) was performed on Thales ($k_f=1.5 \text{ \AA}^{-1}$, Heusler-Heusler, Be Filter on k_f , CRYOPAD). From a standard XYZ polarization analysis we observed magnetic scattering at (0.75,0,0) at T_c , on top of a negative effective baseline (Fig. 3.b). That non-zero baseline is a usual phenomenon in PND, coming from a tiny imbalance in the flipping ratios in polarization channels X, Y and Z. The location of the negative baseline is corroborated by a measurement at (0,0,2.3) which displays the same $|Q|$ value. Notice that the IUC magnetism has never been observed along the (0,0,L) rod, as predicted by the LC model. The full magnetic scattering grows smoothly on cooling down T^* . Then it displays a maximum close to T_c , before dropping down in the SC state. This result could be the first proof of a net interplay between the IUC magnetism and superconductivity. Unfortunately, a leakage in the cryostat and a small piece of tape hidden on the cryostat heat shield jacket deeply affected the experiment (see [20]). Despite our effort to save as much as data we could, the outcome of the experiment is very limited.

2/ Experimental report # 4-02-587

- Experiment part I:

Exp. #4-02-587 is for a continuation of the experiment on Thales with polarized neutrons and CRYOPAD. The purpose was to keep studying the IUC magnetism in an optimally doped $\text{YBa}_2\text{Cu}_3\text{O}_{7-\delta}$. We planned to the exact line shape of the magnetic signal and to determine accurately its T-dependence. Likewise, we also planned to explore the low Q area (**see Part II**), as the decay of the magnetic scattering below T_c could imply a reconstruction of the magnetic pattern (in addition to broken discrete symmetry, the LT invariance can also be broken on cooling down).

We used the same sample as for Exp. # 4-02-541, a large single crystal of $\text{YBa}_2\text{Cu}_3\text{O}_{6.9}$ (a few g) without green phase successfully grown by Pr. Xin Yao at the school of Physics and astronomy of the Shanghai University, by top-seeded solution growth process. The sample is free from the Y_2BaCuO_5 impurity (green phase), which exhibits an antiferromagnetic order below 28 K and low energy paramagnetic response screening the detection of IUC magnetic fluctuations.

The sample was aligned in the (100)/(001) scattering plane, such that wave vector (H,0,L) were accessible. The sample was installed into the orange cryostat dedicated to CRYOPAD. Elastic measurements were performed with a final neutron wave vector $k_f=1.5 \text{ \AA}^{-1}$. A Be filter was inserted in the scattered beam to remove higher order contaminations.

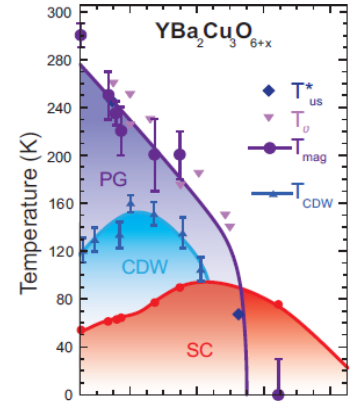


Figure 1: Phase diagram

The quality of the polarization set-up was tested using a quartz sample. The background produced by the sample environment was measured separately and subtracted to the quartz data. Fig. 2 show the variation of the Flipping Ratio (FR) for a typical H-scan. The FR appears rather stable as a function $|Q|$. Furthermore, FR was measured on two different nuclear Bragg scattering for the three orthogonal neutron polarizations X, Y and Z. On (1,0,0), FR is 27 for the 3 polarizations. On (0,0,4), it takes the values 23,21,22, respectively.

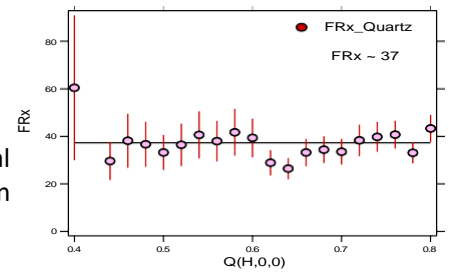


Figure 2 Flipping ratio for a quartz sample at room temperature

Fig. 3.a shows the T-dependence of the spin flip (SF) intensity measured (0.725,0,0) in the X channel. At selected In temperature, the SF intensity was measured for the three X,Y,Z polarizations. A full polarization analysis allows one to extract the SF

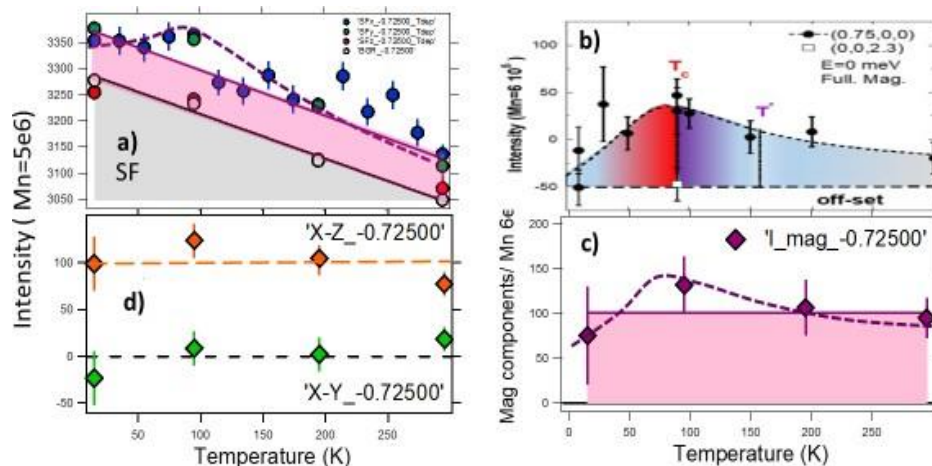


Figure 3 a) temperature dependence of the SF intensity measured at (0.725,0,0) in different polarization channels: X (blue), Y (green), Z (red). The SF background deduced from; XYZ polarization analysis is reported in grey. b) Full magnetic scattering at (0.75,0,0) from the previous measurement. c-d) temperature dependencies at (0.725,0,0): full magnetic scattering (purple), in-plane magnetic component (orange) and out-of-plane magnetic component (green).

background (grey dots in Fig. 3.a), the full magnetic scattering (purple data in Fig. 3.c) and the in-plane and out-of-plane magnetic components (orange and green data in Fig. 3.d). In Fig. 3.a, a net magnetic signal appears on top of a sloping background. In the scattering of points, it is hard to tell whether the magnetic signal is constant or if it could change across T_c as suggested by earlier results (Fig.3.b). Focusing on the full magnetic intensity deduced from XYZ polarization analysis the negative base line (Fig.3 b) in the previous data is absent (Fig.3 c) in the new data set, consistent with a flipping ratio independent of the neutron polarization direction. The magnitude of the magnetic intensity is also consistent between the two experiments. Unfortunately, one cannot characterize accurately the T-dependence of the magnetic signal. Nevertheless, the full polarization reveal that the magnetic scattering mainly comes from magnetic moment aligned in the CuO_2 layer (Fig.3. d).

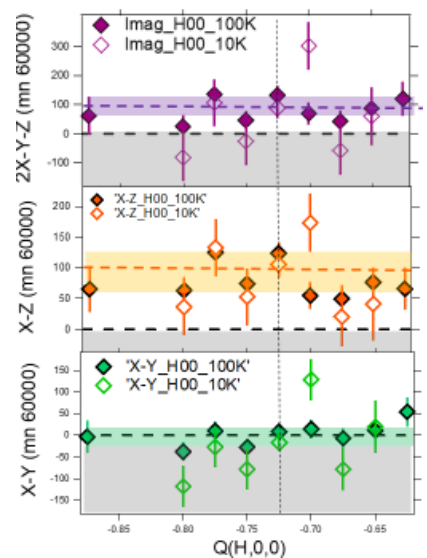


Figure 4 Magnetic scatterings at 10 K and 100 K along (H,0,0) : full magnetic scattering (purple), in-plane magnetic component (orange) and out-of-plane magnetic component

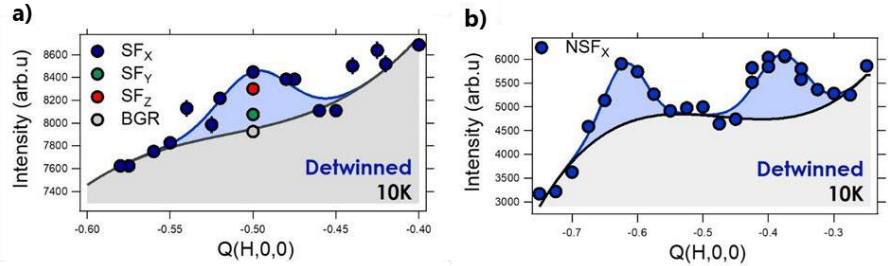
Fig. 4 shows H-scans from $H=0.6$ up to $H=0.9$, measured at 10 K in the SC state and 100 K just above T_c . The magnetic intensity comes in the in-plane magnetic components (labeled X-Z, Fig. 4.b). The magnetic scattering remains almost H-independent in the studied momentum range and does not display any significant change within error bars when going from 10 K to 100 K.

Combining all data, our polarization neutron diffraction study reveals a magnetic scattering widely spread in Q and rather constant in temperature. This signal comes from in-plane magnetic moments. Further work is needed to understand the nature and relevance of such a magnetism for superconducting cuprates

- Experiment part II:

The second part of the experiment was dedicated to the study of the low Q region in a detwinned $\text{YBa}_2\text{Cu}_3\text{O}_{6.6}$ co-aligned array of single crystals grown by the group of Pr. Bernhard Keimer (Max Planck Institute for Solid State Research, Stuttgart). The sample was aligned in the (100)/(001) scattering plane and the experiment carried in the same conditions as for the part I.

Figure 5. Raw data scans along the $(H,0,0)$ line in the YBCO-d sample in (a) the spin flip ($\text{SF}_{x,y,z}$) channel. The background (BGR) is extracted from XYZ-PA. Lines are guide to the eye. (b) Same scan in the NSF_x channel.



Our measurements revealed a static magnetic response at the planar wavevector $\mathbf{q}=(0.5,0)\equiv(\pi,0)$ at low temperature as shown by the longitudinal H-scan in the SF_x channel (Fig.5.a). The same scan in the NSF_x channel (Fig. 5.b) reveals two nuclear peaks $\mathbf{q}_{\text{ch}} = (H \pm 0.125, 0, 0)$, inherent to the Ortho-VIII oxygen ordering of the CuO chains in that YBCO sample, which leads to a nuclear contribution where no magnetic signal occurs. The absence of magnetic scattering at the characteristic \mathbf{q}_{ch} positions confirms the CuO_2 planes as the origin of the magnetic response at $H = 0.5$.

On cooling down from room temperature, the magnetic signal settles in at T^* (Fig.6.a), the PG and IUC magnetism onset temperature highlighting that the $\mathbf{q}=0$ and $\mathbf{q}=\pi$ magnetism may share a common origin. The orientation of the corresponding magnetic moment decomposes into a leading out of plane magnetic component (Fig.6.b) that follows an order parameter like temperature dependence and a flat in-plane magnetic component (Fig. 6.c). The $\mathbf{q}=\pi$ magnetism remains at short range with correlation lengths of $\sim 25\text{\AA}$ in plane (about 5-6 unit cells) [21].

Our measurements further show that at low temperature, the L-dependence of the magnetic signal peaks at $L=0$ with no contribution at $L=0.5$. Interestingly, an additional magnetic signal further shows up at $L=0.5$ above T_c ($\sim 61\text{K}$), with a magnetic moment orientation mainly pointing in-plane (unlike the $L=0$ signal mostly pointing out of plane [21]). The signal vanishes upon heating up to 300K on cooling down below T_c highlighting possible correlations developing at $T > T_c$ (Fig.7.a). This new magnetism may be sensitive to the various electronic states present in the phase diagram.

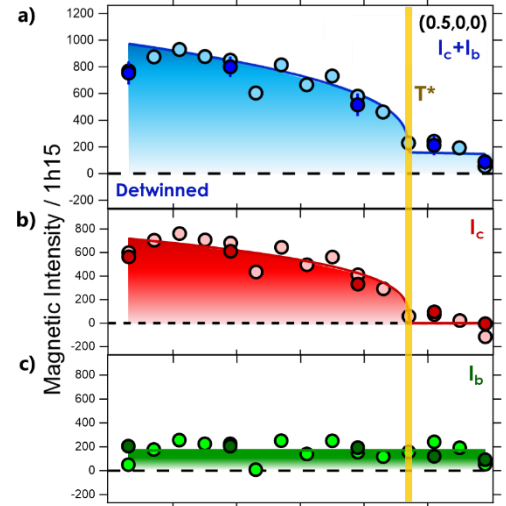
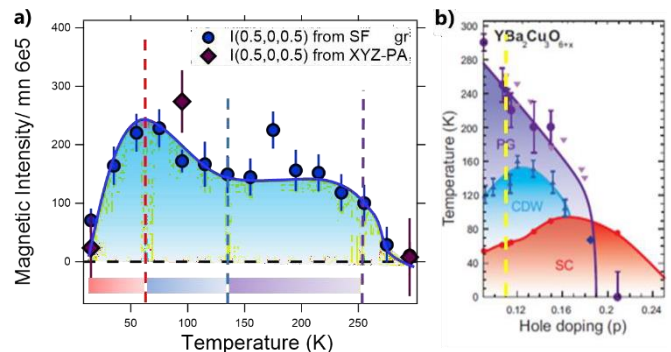


Figure 6. Temperature dependence of the biaxial magnetism in twin-free $\text{YBa}_2\text{Cu}_3\text{O}_{6.6}$ [21] measured at $(0.5,0,0)$: (a) full magnetic scattering; (b) out-plane magnetic scattering; (c) in-plane magnetic scattering.

Figure 7. (a) Temperature dependence of the magnetic scattering at $(0.5,0,0.5)$, measured on Thales TAS and extracted from both XYZ-PA, and the difference between the SF_x signal and background given by XYZ-PA ($\text{SF}_y+\text{SF}_z-\text{SF}_x$). The magnetic scattering may vary in the different electronic states reported in the phase diagram (c): pseudo-gap (PG), incipient charge density wave (CDW) and superconductivity (SC). c) Solid and dashed lines suggest marked or smooth changes when entering the different electronic states.



References:

- [1] R. Daou et al., Nature 463, 519 (2010)
- [2] M.J. Lawler et al., Nature 466, 347(2010)
- [3] Y. Sato et al., Nat. Phys. 13, 1074 (2017)
- [4] H. Murayama et al., arXiv:1805.00276
- [5] L. Zhao et al., Nat. Phys. 13, 250 (2017)
- [6] A. Kaminski et al., Nature 416, 610 (2002)
- [7] J. Xia et al., Phys. Rev. Lett. 100, 127002 (2008).
- [8] B. Fauqué et al., Phys. Rev. Lett. 96, 197001 (2006).
- [9] Y. Li et al, Nature 455,372, (2008)
- [10] C. Varma, Phys. Rev. B 73, 155113 (2006)
- [11] P. Bourges et al., C. R. Physique, 12, 461, (2011).
- [12] Y. Sidis et al., Journal of Physics: Conference Series,449, 012012 (2013).
- [13] L. Mangin-Thro et al., Phys. Rev. Lett. 118, 097003 (2017).
- [14] H.A. Mook et al., Phys. Rev. B 020506(R) (2008).
- [15] Y. Tang et al., arXiv 1805.02063
- [16] Jiang Zhang et al., Science Advances 4, eaao5235 (2018)
- [17] A. Pal et al, Phys. Rev. B 97, 060502 (2018)
- [18] Y. Itoh et al., Phys. Rev. B 95, 094501 (2017).
- [19] L. Mangin-Thro et al., Nat. Comm 6, 7705 (2015)
- [20] Exp. Report 4-02-541
- [21] D. Bounoua et al., accepted in Comm. Phys. arXiv:2111.00525